Applied Surface Science Advances 1 (2020) 100025

Contents lists available at ScienceDirect

Applied Surface Science Advances

journal homepage: www.elsevier.com/locate/apsadv

Inorganic–organic hybrids based on sepiolite as efficient adsorbents of caffeine and glyphosate pollutants

Hugo Baldan Junior[a], Evane da Silva[a], Michelle Saltarelli[a], Denise Crispim[a], Eduardo J. Nassar[a], Raquel Trujillano[b], Vicente Rives[b,*], Miguel A. Vicente[b], Antonio Gil[c], Sophia A. Korili[c], Emerson H. de Faria[a], Katia J. Ciuffi[a]

[a] Universidade de Franca, Av. Dr. Armando Salles Oliveira, 201 - Pq. Universitário, 14404-600 Franca, SP, Brazil
[b] GIR-QUESCAT, Departamento de Química Inorgánica, Facultad de Ciencias Químicas, Universidad de Salamanca, 37008 Salamanca, Spain
[c] INAMAT^2. Departamento de Ciencias, Edificio de los Acebos, Universidad Pública de Navarra, Campus Arrosadía, 31006 Pamplona, Spain

ARTICLE INFO

Keywords:
Sepiolite
Glyphosate
Caffeine
Organically modified sepiolite
Clay mineral
Herbicide

ABSTRACT

Sepiolite clay mineral was functionalized with (3-chloropropyl)triethoxysilane (ClPTES) or 3-[tri(ethoxy/methoxy)silyl] propylurea (TEMSPU) alkoxides and tested as adsorbent for herbicide glyphosate and also of caffeine, two pollutants with very different chemical composition. The materials obtained were characterized by X-ray diffractometry, infrared spectroscopy, thermal analysis, scanning electron microscopy and nitrogen adsorption at −196 °C, and submitted to toxicity and desorption tests. Silane functional groups blocked sepiolite active positions, and adsorption occurred within the zeolitic channels and on the surface of the functionalized solids. Caffeine and glyphosate effectively interacted with urea groups from grafted alkoxide, which could lower the mobility of the adsorbed contaminants. Glyphosate adsorbed on functionalized sepiolite derivatives showed low toxicity.

1. Introduction

Industrial and urban growths cause environmental and hazards and energy shortage to sustainable development. Related multi-activities generate numerous pollutants that are released into water and soil, thereby posing a major health threat and potentially causing irreversible damage for future generations [1]. Organic or inorganic emerging contaminants (ECs) are present in many commercial products, such as pesticides, fertilizers, pharmaceuticals, disinfectants, and natural and synthetic hormones. ECs have been detected in aquatic environments in different parts of the World [2], released from industrial wastewater and secretion of non-metabolized drugs by human bodies or animals. Conventional treatment processes cannot completely remove these highly chemically stable and poorly biodegradable ECs, which often escape intact from conventional sewage treatment plants [3]. Along time, toxic and persistent ECs can accumulate and become a potential threat to the health of aquatic animals and of human beings [4].

The rapid development of agriculture has increased the need for herbicides. Over the past decade, glyphosate-based herbicides (glyphosate = 2-[(phosphoromethyl)amino]acetic acid) have gained importance mainly by the increase of genetically modified crops, becoming the World's most abundant herbicidal molecule [5]. Global concern on the use of glyphosate has risen after it has been found in aquatic environments from both domestic sewage and industrial wastewater. As glyphosate-based herbicides are systemic and have a broad action spectrum, they can be applied in low syrup volumes as compared to conventional herbicides [6]. This herbicide inhibits the enzyme enolpyruvylshiquimate phosphate synthase (EPSPS), involved in the synthesis of aromatic amino acids, so its inhibition results in plant, fungus, or microorganism physiological detriment or death [7,8]. Glyphosate-based herbicides are marketed as over 150 trademarks with different commercial names in more than 119 countries and are registered for use in over one hundred crops [7]; approximately 128 million kg were used in the US in 2016 [9].

Glyphosate flows preferentially in microporous structured soils (i.e., clayey soils), being directed to drainage systems and provoking extensive contamination [10]. In some cases, glyphosate concentrations in surface waters exceeds the maximum level of contaminants (MCL) allowed in drinking water, 700 μg/L according to the US environmental standards, which are less strict than the EU standards, 0.1 μg/L [10,11]. The half-lives of glyphosate and its major metabolite, aminomethyl phosphonic acid, are 0.8–151 and 10–98 days, respectively [7], and degradation half-life of glyphosate in soil has been reported to be 7–60 days [12], showing that it can be classified as persistent. On the other hand, 140 groundwater samples taken in Catalonia, Spain, were anal-

* Corresponding author.
E-mail address: vrives@usal.es (V. Rives).

https://doi.org/10.1016/j.apsadv.2020.100025
Received 29 May 2020; Received in revised form 20 August 2020; Accepted 1 September 2020

ysed in a large study on the concentration of this pollutant in real effluents. Roughly 40% of samples analysed contained glyphosate. Although the mean concentration in groundwater was small (mean concentration 200 ng/L), higher concentrations were found where groundwater samples were taken during a period of heavy precipitation that followed earlier periods of drought, suggesting leaching from soil [13].

According to the World Health Organization [14] the oral LC_{50} of pure glyphosate in rats is 4.230 mg/kg, while the manufacturer (Monsanto©) cites 5.600 mg/kg. The acute toxicity of this pesticide is considered low but may harm enzymatic functions in animals [15,16]. When injected into the abdomen of rats, this pesticide decreased the activity of some enzymes.

Caffeine (1,3,7-trimethylxanthine) is an alkaloid belonging to the methylxanthine family and also a major contaminant, widely used as a stimulant and also as a biological marker for pollution detection [17–19]. Large amounts of caffeine are located in seeds, leaves, and fruits of some plants, wherein they act as a natural pesticide that paralyzes and kills certain insects that feed on these plants. Humans most commonly consume caffeine in infusions extracted from coffee plant seeds and teas made from the leaves of some herbs, as well as in various foods and beverages containing products derived from some species of cola nuts. Caffeine acts as a stimulant of the human central nervous system, temporarily warding off drowsiness and restoring alertness; even moderate consumption over the years may have a mild positive effect against some diseases, including Parkinson, heart disease, and certain cancers [20]. In human beings, hepatic cytochrome P450 partially metabolizes dietary caffeine through oxidative N-demethylation and/or ring oxidation, to produce theophylline (1,3-dimethylxanthine), paraxanthine (1,7-dimethylxanthine), 1,3,7- trimethyluric acid and other by-products [21], which are excreted in urine along with un-degraded caffeine. Microorganisms in wastewater cannot satisfactorily metabolize caffeine, which makes it a chemical marker of surface water pollution. Li et al. have reviewed the highest concentration of caffeine in wastewater. A surprisingly high value of 3594 μg/L was found in Singapore wastewater, while much lower values have been reported for Jundiaí River Brazil (19.3 μg/L), river waters in Lebanon (10.2 μg/L) or raw drinking water from Aksaray, Turkey (3.39 μg/L) [19].

Environmental remediation requires new materials consisting of solid matrixes that can act as active, selective and recyclable heterogeneous catalysts for ECs degradation. Nanocomposite materials can help to overcome the pollution problems related to ECs. Sepiolite, $Mg_8Si_{12}O_{30}(OH)_4(H_2O)_4.8H_2O$, is a fibrous, hydrated magnesium silicate. It resembles porous structures such as zeolites and mesoporous silicas, with a high specific surface area, and excellent adsorption properties [22]. Currently, its industrial applications are diverse and are based on its ab/adsorptive properties. For instance, sepiolite can absorb 2.5 times its mass in water, which underlies the great plasticity of the clay/water system [23]. Functionalization by alkoxides increases the number of active sites for chemical bonding, enhancing its adsorptive capacity [24].

Recently, new methods for organoalkoxide immobilization on clay surfaces have been developed in order to overcome some drawbacks associated with conventional methods [25]. Depending on the reaction conditions, chemistry of the organoalkoxide and surface previous history, a number of different structures can be produced on the surface, and the choice of the preparation methodology is a key step for Materials Science, Environmental Chemistry and Industrial Chemistry. The following synthesis routes can be cited: i) to use an excess of alkoxide without solvent [26], ii) to use nonpolar solvents and limited amounts of alkoxide [27], iii) to use polar solvents with limited amount of silane [28–31], iv) microwave-assisted synthesis [32]. The use of the silane in the presence of the clay mineral without any solvent is highlighted according to literature data [27], especially to prepare adsorbents; this method guarantees that the alkoxide will be effectively attached to the clay surface and decreases the hydrolysis of the alkoxide (if using inert atmosphere), which is in turn drastically favored in aqueous suspension, with precipitation of organosilica without effective grafting onto the surface. In aqueous solution, the basic steps of hydrolysis and condensation reactions are hardly controlled without the use of stabilizing agents, promoting the precipitation of organosilica and resulting in conventional composites formed by a hybrid mixture of silica and sepiolite fibers. As a result, the distribution of the organic groups on the sepiolite surface may be strongly heterogeneous, leading to poorly adsorbing solids. Hence, the critical points are: (i) to understand the role of the functional groups present on the organo-alkoxides and their ability to act as efficient active sites for adsorption, and (ii) to know how these groups could affect the grafting effectiveness on sepiolite fibers and the behavior of the obtained material during adsorption/desorption cycles of different contaminants, as it is desirable to maintain the structural stability of the alkoxide during adsorption.

As indicated, caffeine and glyphosate have very different chemical structures (Scheme S1, Supplementary Data), glyphosate showing various polar –OH groups (one of them actually –COOH). For this reason, their interaction with silane-functionalized sepiolite adsorbents deserves a comparative study. The choice of the sepiolite grafting methodology was conditioned by the application of the final solids as adsorbents, looking for active sites homogeneously distributed on the surface of the sepiolite fibers, and for an easy separation after adsorption experiments. Thus, aggregation of sepiolite fibers should be avoided for a better accessibility to the solid. In addition, the presence of organic groups on the surface could induce a different adsorption strategy, not controlled exclusively by the value of the specific surface area.

The functional groups existing on the organosilanes, chloropropyl and propylurea groups, were selected due to their ability to bond with contaminants via electrostatic and hydrogen bonds, respectively. We have used two different alkoxides, namely, (3-chloropropyltriethoxysilane (ClPTES) and 3-[tri(ethoxy/methoxy)silyl] propylurea (TEMSPU)), grafted on sepiolite surfaces to adsorb organic pollutants (caffeine and glyphosate), aiming to improve the adsorption performance by means of the mobility of contaminant, the time required for adsorption equilibrium, and the amount adsorbed; to our best knowledge, their use for these purposes has not been previously reported.

Thus, in this work, a sepiolite clay was functionalized with ClPTES or TEMSPU alkoxides. The prepared materials were characterized by powder X-ray diffraction (PXRD), Infrared absorption spectroscopy (FT-IR), Thermal analysis (TA), Scanning Electron Microscopy (SEM) and nitrogen adsorption/desorption at −196 °C, and submitted to toxicity and desorption tests. The materials were then applied as adsorbents of two pollutants with chemical structures very different, namely caffeine, considered as a probe molecule, and the widely used herbicide glyphosate (N-(phosphonomethyl)glycine).

2. Experimental procedure

2.1. Materials

Natural sepiolite from Vallecas (Madrid, Spain), commercially available as PANGEL®, and kindly supplied by TOLSA, S.A. (Madrid, Spain), was used in this work. The natural clay was purified by the dispersion-decantation method, obtaining a very pure clay material (Fig. 1), which was used after drying at 60 °C (hereafter denoted as *Sep*). This clay mineral, functionalized with a silane, has been recently used by us for adsorption of cationic and anionic dyes [26].

All reagents and solvents (from Merck or Aldrich) were of high purity commercial grade, and most of them used as received. High purity (>99 %) glyphosate and caffeine were used also as received.

2.2. Preparation of organically functionalized sepiolite

Purified sepiolite was reacted with alkoxides 3-chloropropyltriethoxysilane (ClPTES) or 3-[tri(ethoxy/methoxy)silyl]propylurea (TEMSPU), using a mass of 10.0 g of Sep for 50.0 mL of ClPTMS or

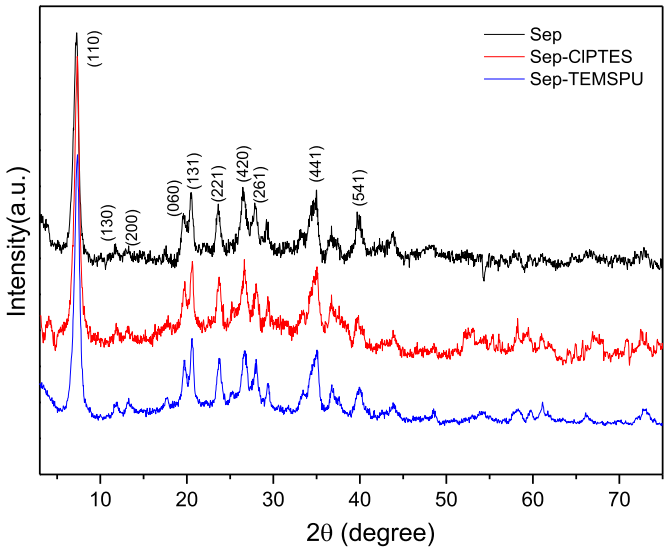

Fig. 1. XRD patterns of Sep, Sep-ClPTES and Sep-TEMSPU solids.

TEMSPU. The suspension was heated at 180 °C for 48 h under magnetic stirring in a refluxing system under argon atmosphere (without using any solvent, as alkoxides are liquids). The resulting solids were washed with ethanol for 24 h in a Soxhlet system, and additionally 5 times with water, and then were oven-dried at 85 °C for 24 h. These solids were denoted as *Sep-ClPTMS* and *Sep-TEMSPU*, respectively, depending on the alkoxide used.

2.3. Characterization techniques

The powder X-ray diffraction (PXRD) diagrams of the solids were recorded in a Miniflex II-Rigaku diffractometer operating at 40 kV and 30 mA, using filtered Cu Kα radiation in the 5–70° (2θ) range. All the analyses were carried out at a scan speed of 5° (2θ)/min.

The specific surface areas were determined by the Brunauer–Emmer–Teller (BET) method [33] from the corresponding nitrogen adsorption isotherms recorder in a Micrometrics ASAP 2020 physical adsorption analyzer at −196 °C. The samples (ca. 0.2 g) had been previously degassed for 4 h at 150 °C at a pressure lower than 50 μmHg. The external surface area (S_{ext}) was estimated using the t-plot method [33]. The total pore volume (V_{PT}) was calculated from the amount of nitrogen adsorbed at a relative pressure of 0.99 [33].

The FT-IR spectra were recorded in the 4000–350 cm^{-1} range in a Perkin-Elmer Spectrum One equipment, using the KBr pellet technique, with 32 scans to improve the signal-to-noise ratio, and a nominal resolution of 4 cm^{-1}; about 1 mg of sample and 300 mg of KBr were used in the preparation of the pellets.

The thermal analysis were carried out in a TA Instruments SDTQ600 simultaneous differential thermal analysis and thermogravimetric analysis (DTA-TG) thermal analyzer, in the temperature range from 25 to 900 °C, at a heating rate of 20 °C/min and under air flow (100 mL/min). The differential thermogravimetric analysis (DTG) curves have been also plotted.

For recording the scanning electron microscopy (SEM) images, a VEGA 3 SBH – EasyProbe model, from TESCAN, equipment was used. The samples were first coated with a thin gold film.

The point of zero charge (pH_{ZPC}) was determined by using flasks with 20 mg of sample in 20 mL of a 0.1 mol/L NaOH solution. The initial pH was adjusted with 0.1 mol/L of HCl or NaOH solution to twelve various values (1–12). The solutions were stirred for 24 h at room temperature and then centrifuged to remove the supernatant liquid, and the final pH of the solutions was determined [34].

2.4. Adsorption procedure

Copper-glyphosate complex (GLY) or caffeine (CAF) concentration in the solutions was determined in a Hewlett-Packard 8453 Diode Array UVvis spectrophotometer, 1 cm path length cell, at the absorption maxima of 248 and 276 nm, respectively. Previously, their linear concentration dependence was verified in all the concentration range used in the experiments, according to the Beer–Lambert law.

To measure the adsorption kinetics of the pollutants onto the adsorbents, 5.0 mL of solutions with an initial concentration of 25 mg/L for CAF and 300 mg/L for GLY was introduced into the glass vials and mixed with 0.05 g of Sep, Sep-ClPTMS or Sep-TEMSPU. The suspensions were stirred continuously at room temperature. At predetermined time intervals between 1 and 1500 min, the pollutant concentration in the supernatant was analyzed, after previous separation of the solid phase by centrifugation at 3000 rpm, allowing to calculate the amount of pollutants adsorbed onto the solids. The adsorbed amount of the pollutant (q_t) was calculated according to Eq. (1):

$$q_t = \frac{(C_i - C_t) \cdot V}{m} \quad (1)$$

where q_t is the amount adsorbed (mg/g) at time t (min), C_i the initial CAF and GLY concentration in the solution (mmol/L), C_t the CAF and GLY concentration (mg/L) in the solution at time t, V the volume of the solution (L), and m the mass of adsorbent (g). All experiments were conducted in duplicate.

2.5. Desorption experiments

The solids obtained from equilibrium studies, that is, containing adsorbed GLY or CAF, were magnetically stirred for 1500 min at 25 °C using distilled water, aqueous sodium chloride (0.1 mol/L), or methanolic sodium chloride (0.1 mol/L) for GLY, and distilled water, absolute ethanol, aqueous sodium hydroxide (0.02 mol/L), or hydrochloric acid (0.02 mol/L) for CAF. After contacting with these extraction solutions, the samples were centrifuged at 3000 rpm and the supernatant liquid analyzed by UV–vis spectroscopy. All experiments were conducted in duplicate. The amounts of desorbed pollutants were referred to the amounts adsorbed during the adsorption equilibrium process.

2.6. Cytotoxicity assay

The cytotoxic effects were studied by determining the cell viability monitoring the growth of untreated and treated cells using the Cell Proliferation Kit (an XTT-based colorimetric assay, Roche, Mannheim, Germany). The normal human lung fibroblasts (GM07492A cells, Banco de Células do Rio de Janeiro-BCRJ, Rio de Janeiro, Brazil) were used. The cells were maintained as monolayers in plastic culture flasks (25 cm^2) containing Ham-F10 + DMEM (Sigma-Aldrich) culture medium supplemented with 10% fetal bovine serum (Nutricell), antibiotics (0.01 mg/mL streptomycin and 0.005 mg/mL penicillin; Sigma-Aldrich), and 2.38 mg/mL HEPES (Sigma-Aldrich). The cultures were maintained at 37 °C under 5% CO_2. For these experiments, the cells (10^4 cells/well) were placed onto 96-well microplates. Each well received 100 μL of HAM F10/DMEM medium containing glyphosate, sepiolite, sepiolite + ClPTES, sepiolite + TEMSPU, sepiolite + ClPTES + glyphosate, and sepiolite + TEMSPU + glyphosate. The tested concentrations ranged from 1.2 to 5000 μg/mL. The negative (without treatment), solvent (DMSO 1%; Sigma), and positive (DMSO 25%) controls were included. After incubation at 37 °C for 24 h, the medium was removed, and the cells were washed with 100 μL of PBS and exposed to 100 μL of HAM-F10 medium without phenol red. Then, 25 μL of XTT was added to each well. The microplates were covered and incubated at 37 °C for 17 h. The absorbance of the samples was determined by using a multiplate reader (ELISA – Asys – UVM 340/Microwin 2000) operating at a test wavelength of 450 nm and a reference wavelength of 620 nm. The cytotoxic activity was assessed by using the parameter of 50% inhibition of

Table 1
Textural properties of the samples.

Sample	S_{BET} (m^2/g)	S_{ext} (m^2/g)	V_{PT} (cm^3/g)	pore size (nm)
Sep	245	144	0.631	103
Sep-ClPTES	100	81	0.362	14.6
Sep-TEMSPU	100	82	0.359	14.4

cell line growth (IC_{50}), the concentration of inhibitor in the cell culture medium, required to inhibit a protein's transporting activity by 50% [35]. LC_{50} is the concentration of the compound in feed (or water in case of cells) that is lethal for 50% of exposed population [36]. The experiments were repeated three times.

3. Results and discussion

3.1. Characterization of the solids

The diffractograms of functionalized sepiolite are shown in Fig. 1. As previously reported [25,37], Sep organofunctionalization with APTES or TEMSPU did not significantly change the Sep structure because this clay mineral has a non-swellable structure. The basal value calculated from their characteristic (110) X-ray reflection (2θ = 7.4°) remained practically unchanged, 12.2 Å, for all three samples, indicating that the purification and functionalization processes preserved the characteristic Sep fiber crystallinity.

The values for specific surface areas (S_{BET}), external surface areas (S_{ext}) and total pore volumes (V_{PT}) of the functionalized materials, determined from the nitrogen adsorption results, are summarized in Table 1. Data for purified Sep are also included for comparison. The adsorption isotherms corresponded to type II, with H3 type hysteresis loops (Fig. S1) according to the IUPAC classification [38] when nitrogen adsorption-desorption are carried out, features typical of this clay mineral. The initial part of the adsorption isotherm was attributed to monolayer-multilayer adsorption. Type H3 hysteresis loops are generally observed in adsorbents containing aggregated plate-like particles, such as fibrous or layered and also pillared clay minerals, which give rise to slit-shaped pores [26]. For a microporous solid, BET surface area could be related to the sum of the micropore surface area and the external surface area, which, as indicated, was calculated from the *t*-plot. The specific surface area of Sep, 245 m^2/g, is typical for this clay mineral, 144 m^2/g corresponded to external surface area and, consequently, the micropore surface area being 101 m^2/g, in accordance with the channel structure of this solid. After functionalization, the specific surface area decreased to 100 m^2/g for both Sep-ClPTES and Sep-TMSPU, most of them (81–82 m^2/g) corresponding to external surface area and the micropore surface area being consequently very low. These results are in agreement with previous results [26], suggesting that the organic groups functionalized onto the clay surface blocked the access of nitrogen molecules to the sepiolite pores, that is, the functionalizing organic matter should block the entrance to sepiolite channels. Some authors have reported that, at the same time, these organic groups may form new compartments and/or increase the number of existing compartments for gas adsorption [39,40].

The FTIR spectra of the solids are shown in Fig. 2, and the assignments of the signals is summarized in Table S1. The stretching of –OH groups bonded to octahedral Mg cations were recorded as bands at 3560–3562 cm^{-1}, while the vibrations from water molecules appeared at 3336 (O–H stretching) and 1660 (bending) cm^{-1} [15, 41]. The broad band close to 1000 cm^{-1} corresponded to the Si–O–Mg–O–Si vibrations, while the vibrations involving Si–O and Mg–O bonds were also recorded at lower wavenumbers. The functionalized solids showed the stretching vibrations of C–H bonds at 2930 cm^{-1} (Sep-TEMSPU) and 2979 cm^{-1} (Sep-ClPTES), while the characteristic bands from CH_3 stretching vibrations appeared at 2821 and 2838 cm^{-1}. The region between 2000

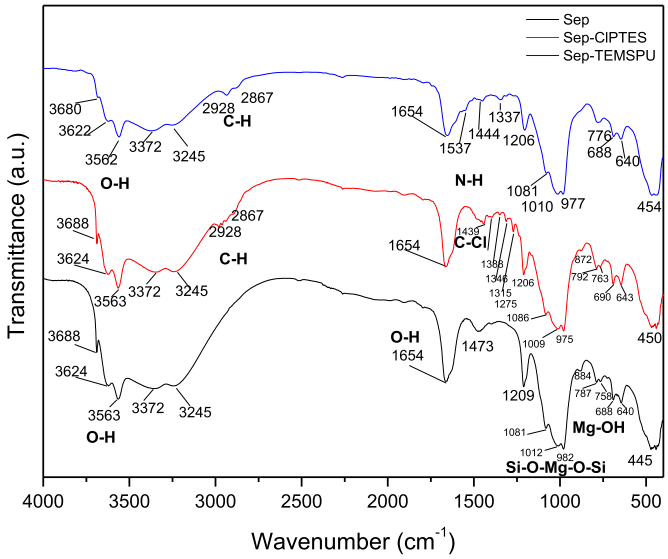

Fig. 2. Infrared spectra of Sep, Sep-ClPTES and Sep-TEMSPU solids.

and 1200 cm^{-1} has been commonly used to identify the presence of organic molecules interacting with fibrous silicates [42]. The N–H deformation vibrations were recorded in the 1500–1550 cm^{-1} range, while C–H strain vibrations, possibly interacting to Si–OH bonds, were observed between 1290 and 1448 cm^{-1} and between 1272 and 1439 cm^{-1}, respectively. The band close to 1069 cm^{-1} corresponded to the Si–O–Si and Si–O–Si–C groups and the band at 698 cm^{-1} can be assigned to the stretching of the C–Cl bond [43]. The intensities of the bands in the high wavenumber region decreased as a result of the condensation of silanes with hydroxyls from Mg–OH or Al–OH groups from the fibrous structures.

On comparing the characteristic sepiolite bands in the spectrum of the parent solid and those for the functionalized samples, it is deduced that the functionalizing molecules interacted with the clay particles via their hydroxyl groups [27]. The incorporation of the organic molecule affected the vibration of the stretching vibration of hydroxyl groups in Si–OH and Mg–OH units, at 3693 and 3560 cm^{-1}, particularly in the case of TEMSPU, while the shift of this band was less evident in the case of the Sep-ClPTES sample. The band at 869 cm^{-1} disappeared for Sep-TMSPU and showed very low intensity for Sep-ClPTES, indicating that it participated in the bonding with the silane. This band has been assigned to hydroxyl groups bonded to Fe^{3+} cations, present in small amounts in the sepiolite [44].

The TG curve for Sep-TMSPU showed five mass loss steps (Fig. 3). The first one, at 69 °C (mass loss 6%), was assigned to water elimination. The second and third ones, at 221 (9.0%) and 334 °C (10.0%), were assigned to removal of zeolitic water and to the beginning of decomposition of TMSPU moieties, respectively. Two effects were observed at high temperature, at 656 (3.0%), assigned to decomposition of residual organic matter from TMSPU and folding of the structure following the loss of coordinate water, and 825 °C (2.0%) assigned to dehydroxylation of Sep and perhaps removal of residual carbon content [45,46]. The total mass loss assigned to alkoxide removal was close to 27%, confirming the large extent of functionalization. The functionalizing molecules were not completely removed during heating, as a portion remained on the solid particles forming amorphous silica. The amount of TMSPU fixed by unit cell of the clay minerals was calculated from the mass loss between 110 and 500 °C, considering the hydrolysis and condensation of one, two or three silanol groups onto the fibrous clay minerals; the average stoichiometry was Sep-$TMSPU_{0.265}$ (formula of Sep referred to 6 Si atoms).

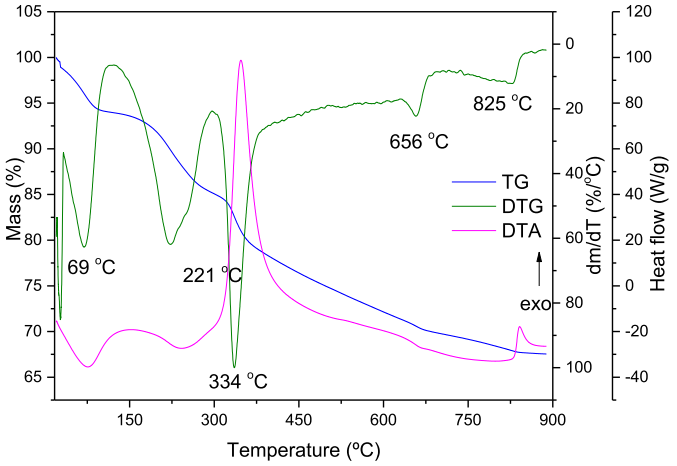

Fig. 3. Thermoanalytical curves (TG, DTG, DTA) for Sep-TEMSPU solid material.

Table 2
Pseudo-first- and -second-order parameters for caffeine (CAF) and glyphosate (GLY) adsorption by modified sepiolites[a].

	CAF		GLY	
	Sep	Sep-TEMSPU	Sep-TEMSPU	Sep-CIPTES
First-order				
k_1 (1/min)	1.43	0.063	0.13	0.21
χ^2	0.70	0.76	51	14
R	0.92	0.94	0.85	0.96
Second-order				
k_2 (g $^{-1}$mg•min)	0.91	0.049	0.023	0.034
χ^2	0.33	0.27	28	14
R	0.97	0.98	0.92	0.96

[a] First-order, $q_t = q_e \cdot (1 - \exp(-k_1 \cdot t))$; Second-order, $q_t = \frac{k_2 \cdot q_e^2 \cdot t}{1 + k_2 \cdot q_e \cdot t}$; where q_e and q_t (mg/g) were the amounts of solute adsorbed at equilibrium and at a certain time, t, respectively, k_1, and k_2 were the reaction rate constants of pseudo-first and pseudo-second-order rate, respectively.

The SEM images of purified Sep revealed a fibrous morphology, which was retained even after functionalization (Fig. 4), although formation of small agglomerates was observed. These fibers had flat or straight shapes and were randomly oriented in aggregates. After grafting with ClPTES and TEMSPU, larger aggregates with preferential orientation were observed, which formation is probably favored by the organic groups that may maintain the fibers grouped via hydrogen bonding (amine from urea and magnesium hydroxyl groups), or hydrophobic interactions from propyl chains on the sepiolite surface. Usually, surface stabilization mechanisms in fiber nanoparticles favor particle aggregation; the presence of silane groups allowed the functionalization of particles with organic groups, which could generate their breakdown. However, as reported by Chen et al. [47] and by Suárez and García-Romero [48], sepiolite functionalization increases fiber aggregation due to the formation of a polymer-like film that maintained the fibers aggregated.

3.2. Kinetic and equilibrium studies of adsorption

The pH_{PZC} values were 7.0, 7.0 and 7.2 for Sep, Sep-ClPTES and Sep-TEMSPU, respectively. Lazarevic et al. [49] observed that the point of zero charge of natural sepiolite was 7.4, decreasing to 7.0 when functionalizing with N-[3-(trimethoxysilyl)propyl] ethylenediamine trisodium acid (MSEAS), but considering that this difference was negligible. It is assumed that when the pH of the solution is higher than the pH_{PZC} of the solid material, its surface is negatively charged and, analogously, when the pH of the solution is lower than the pH_{PZC} of the solid material, its surface is positively charged. Thus, cations adsorption is favored on negatively charged surfaces, while anions adsorption is favored on positively charged surfaces. According to literature [50,51], pH_{PZC} is essential to understand the influence of pH on the adsorption process; depending on the solution concentration, the mechanism becomes more efficient. In this sense, GLY presents a zwitterionic behavior, with separation of two charges at neutral pH, one positive on the amino group and one negative on the phosphonate group [52]. Thus, in the present work, the pH of the GLY solution was adjusted to the value 3.0, lower than the pH_{PZC} of the adsorbents, to ensure that their surface would be charged positively and anion adsorption would be favored. Caffeine adsorption experiments were performed at pH=6.

According to the experimental data (Fig. 5), caffeine adsorption onto Sep and Sep-TEMSPU was well defined. In the kinetic study, the maxima caffeine adsorption capacities (q_t) were 2.3 and 2.2 mg/g, respectively, on Sep and Sep-TEMSPU. Sep modification with the alkoxide slightly reduced caffeine adsorption, which can be explained by the relationship between the volume of the Sep pores and of the TEMSPU molecule—the latter is large, so caffeine access to the Sep adsorption sites was not easy, and the maximum caffeine adsorption capacity decreased. The experimental data provided by the kinetic studies on the caffeine adsorption onto Sep and Sep-TEMSPU were adjusted to the pseudo-first- and pseudo-second-order models [18, 53–55], Fig. 5 and Table 2. The pseudo-second-order model describes the chemical adsorption process well: the process involved electron donation or exchange between the adsorbate and the adsorbent through covalent and ionic bonds [18,26, 53,54,56].

In the case of GLY adsorption onto Sep-TEMSPU and Sep-CIPTES, the results are also included in Fig. 5 and Table 2. The maxima GLY adsorption capacities (q_t) on these solids were 15.4 and 13.4 mg/g, respectively. The pseudo-second-order model also described well the chemical adsorption process of the herbicide on the adsorbent. Khenifi et al. [57] reported that glyphosate adsorption onto Ni_2AlNO_3 LDH matrixes also fitted well the pseudo-second-order model, observing that initial adsorption of glyphosate was fast. The equilibrium was reached within 30 min, and the maximum adsorption was 180 mg/g, which demonstrated that not only the adsorbent, but also the interactions between the adsorbent and the adsorbate affected the adsorption process. Li et al. [58] observed a slower initial adsorption when they studied glyphosate adsorption onto MgAl layered double hydroxides, equilibrium being reached only after 150 min. Such differences could be attributed to the influence of the physical properties of the different matrixes on the adsorption process.

In order to evaluate the efficiency of the prepared adsorbents, the adsorption equilibrium as a function of concentration was studied (Fig. 6). From the equilibrium isotherms, it was concluded that the adsorption capacity of Sep adsorbents increased with the increase of the initial caffeine concentration, in which Sep showed a higher adsorption capacity than Sep-TEMSPU. According to Giles classification [59], the shapes of the adsorption isotherms recorded were classified as type L-2. Type L or Langmuir isotherms have a convex, nonlinear slope. In this case, the availability of the adsorption sites decreased with increasing concentration of the solution and subgroup 2 indicated the saturation of the surface where the adsorbate had more affinity for the solvent than the adsorbed molecules, and showed that first layer formation had already occurred, confirming that the isotherms have reached a *plateau*. Therefore, materials adsorbed CAF and GLY effectively. In the case of CAF, Sep provided the highest adsorption, with a q_e(max) value of 54 mg/g and Sep-TEMSPU reached a q_e(max) of 18 mg/g. In the case of GLY, the maximum equilibrium adsorption capacity was 30 mg/g for Sep-CIPTES. Mathematical isotherm equations of Langmuir, Freundlich and Toth were applied to the experimental results [60–62]. It is obvious that adsorption is influenced by functionalization, having a very positive effect in the case of GLY but not in the case of CAF. The presence of silanes seemed to create new active sites for the adsorption of GLY, probably through the OH and NH po-

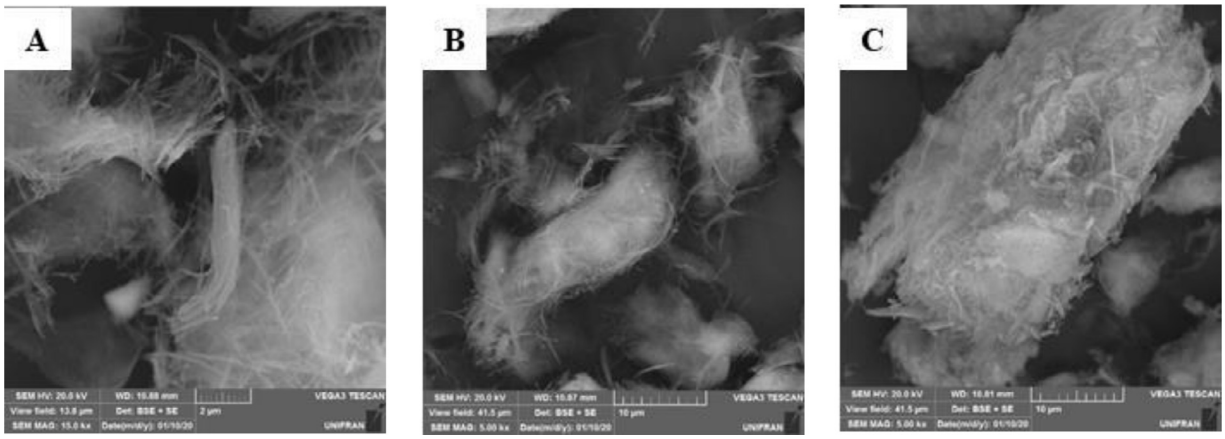

Fig. 4. SEM images of Sep (A), Sep-ClPTES (B) and Sep-TEMSPU (C) solids.

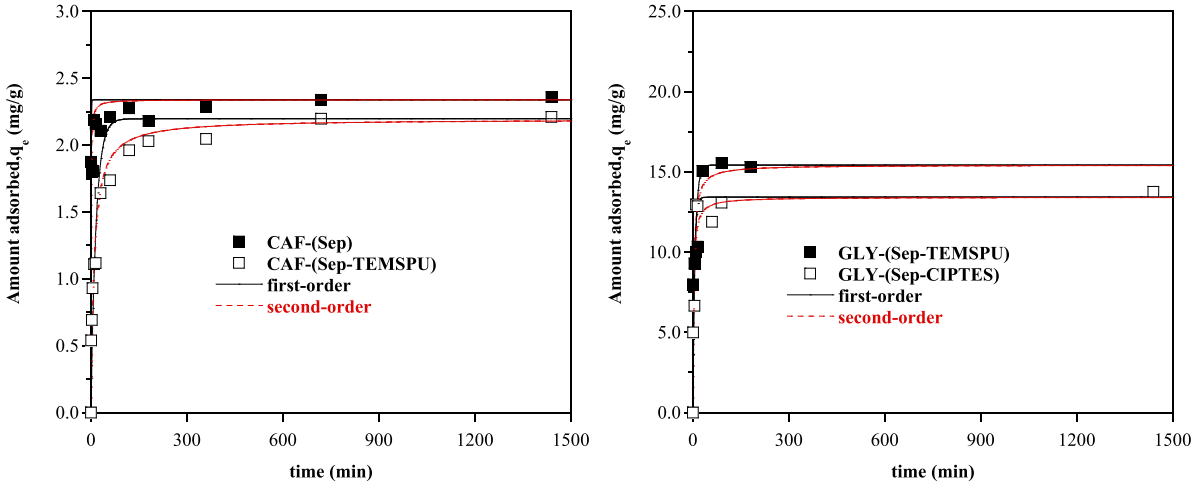

Fig. 5. Kinetic adsorption data for caffeine (CAF) and glyphosate (GLY) adsorption on the modified sepiolites.

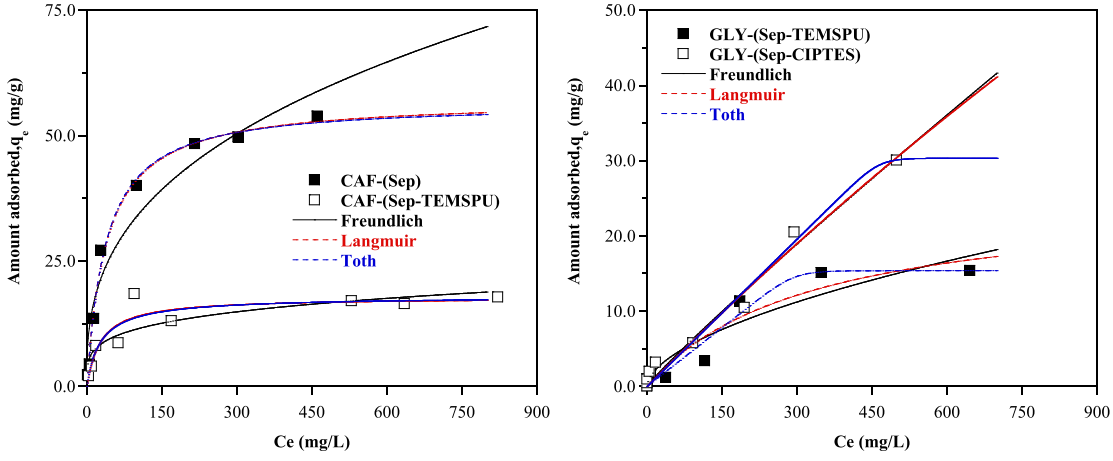

Fig. 6. Experimental (symbols) and model (lines) isotherms for the equilibrium adsorption of caffeine (CAF) and glyphosate (GLY) adsorption on the modified sepiolite adsorbents.

lar groups in this pollutant, while these positions seemed to be non-active for the adsorption of CAF, in which the adsorption decreased, probably because the own silanes occupied the surface of the clay mineral. Nonlinear regression helped to estimate the adsorption parameters for the solids evaluated in this work (Table 3). A comparison with results reported in the literature, in terms of maximum adsorption capacity, is given in Table S2 (CAF) and Table 4 (GLY). Although there is a great variation between the systems, the maximum adsorption values obtained here were in agreement with literature, indicating the adsorption ability of sepiolite-based adsorbents. The non-toxic character of the solids is other relevant factor for their use as adsorbents in the environment.

Table 3
Freundlich, Langmuir and Toth equation parameters for caffeine (CAF) and glyphosate (GLY) adsorption by modified sepiolites.*

	CAF		GLY	
	Sep	Sep-TEMSPU	Sep-TEMSPU	Sep-CIPTES
Freundlich				
k_F (L/g)	6.5	3.8	0.43	0.094
m_F	2.8	4.2	1.8	1.1
χ^2	196	72	37	16
R	0.97	0.87	0.94	0.991
Langmuir				
q_L (mg/g)	57.3	17.8	25.3	324
k_L (L/mg)	0.026	0.037	0.0031	0.0002
χ^2	20	43	26	17
R	0.997	0.93	0.96	0.991
Toth				
q_T (mg/g)	56.4	18.1	15.4	30.3
k_T (L/mg)	0.025	0.041	0.0034	0.0022
m_T	1.1	0.91	12	23
χ^2	20	42	14	15
R	0.997	0.93	0.98	0.991

*Freundlich, $q_e = k_F \cdot C_e^{1/m_F}$; Langmuir, $q_e = \frac{k_L \cdot q_L \cdot C_e}{1+k_L \cdot C_e}$; Toth, $q_e = \frac{k_T \cdot q_T \cdot C_e}{[1+(k_T \cdot C_e)^{m_T}]^{1/m_T}}$; where q_e (mg of adsorbate/g of adsorbent) was the amount adsorbed, C_e (mg/L) was the concentration in solution, k_i the equilibrium constant (k_F) or the binding affinity (k_L, k_T) and m_i characterized the mobility of the molecules adsorbed and the heterogeneity of the system.

At the beginning of the adsorption process, the high number of active sites on the Sep clay surface favored multilayer adsorption, and the same site was able to adsorb two or more glyphosate molecules. After the surface sites were saturated, adsorption started to occur in the internal sites of the Sep structure. As the glyphosate concentration therein was lower, monolayer adsorption was favored. Moreover, the clay zeolitic channels contained zeolitic water, which favored glyphosate solubilization and its adsorption onto the sites.

In general, the results indicated that the matrixes studied herein are potential alternative adsorbents to treat glyphosate-contaminated soils and waters, as well as other emerging contaminants with characteristics similar to those of glyphosate.

3.3. Desorption studies of glyphosate and caffeine

The study of GLY desorption was performed to verify the reusability of the produced matrices. The results obtained in the desorption test for glyphosate using water as solvent and for caffeine experiments considering water, ethanol, 0.02 mol/L NaOH and 0.01 mol/L HCl solutions, are summarized in Table 5. In the case of the glyphosate-copper complex, it was desorbed from Sep, Sep-ClPTES and Sep-TMSPU using water as a solvent due to the lability of this complex, which could be dissociated using acidic or basic solutions. GLY desorption effectively occurred in the case of both Sep-TEMSPU and Sep-ClPTES. The amount of GLY desorbed after 24 h was 81% from Sep-CIPTES, while in the case of Sep-TEMSPU it reached 100%. GLY was extremely water-soluble, which facilitated desorption, and the matrices had a functional adsorptive capacity. Piccolo et al. [69] found that desorption of GLY from different European soils varied from 15% to 80% of the initial amount of adsorbed herbicide, depending on the soil characteristics. This indicated that GLY adsorption onto soils was far from being permanent, and that the herbicide may leach to lower soil layers with biological activity. Morillo et al. [61,67] have shown that the copper-complexed glyphosate molecule favors desorption, as it is quite soluble in the presence of water.

Table 5
Glyphosate (GLY) desorption results.

Adsorbent/GLY amount on solids (mg/g)	Amount desorbed	
	mg/L	%
Sep-ClPTES (111 mg/g)	64.5	57.9
24 h		
48 h	90.5	81.4
72 h	69.1	62.1
Sep-TEMSPU (80 mg/g)	35.8	44.7
24 h		
48 h	80.0	100
72 h	55.2	68.9

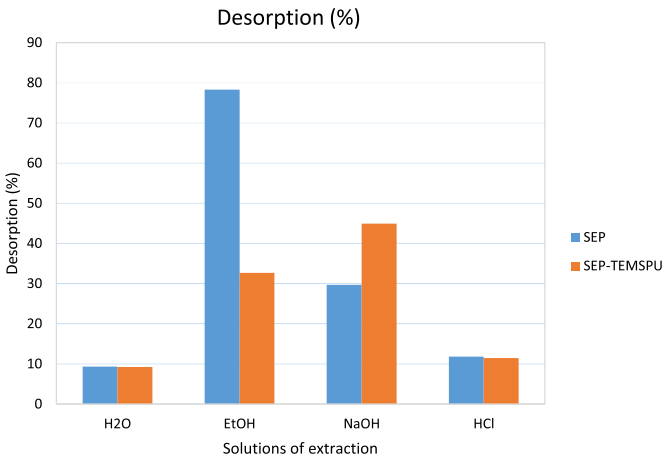

Fig. 7. Desorption in different solvents of the samples Sep and Sep-TEMSPU containing CAF.

Caffeine desorption was investigated using various solvents and the results are summarized in Fig. 7. Ethanol provided better caffeine desorption from Sep because caffeine was very soluble in this solvent. NaOH facilitated caffeine desorption from Sep-TEMSPU, but distilled water and HCl provided small caffeine desorption from both Sep and Sep-TEMSPU. Desorption percentages were good, which evidenced weak physical adsorption, and showed that caffeine recovery was possible.

Table 4
Comparison of the maximum capacity for glyphosate (GLY) adsorption by adsorbent materials.

Adsorbent	q_e (mg/g)	Reference
Biopolymeric membranes (chitosan and alginate)	10.8	[63]
Aluminum sludge	85.9	[64]
Ni_2AlNO_3	180	[57]
Biochar	44	[65]
PANI/ZSN-5 (3 samples)	59.9; 61.9; 98.5	[66]
Soils	38	[67]
Activated carbon	58.4	[68]
Sep-ClPTES	30	This work
Sep-TEMSPU	15.4	This work

Table 6
IC_{50} obtained for GM07492A cell line treated with the different agents.

Treating agent	IC_{50} (μg/mL)
GLY	2262.0±148.2
Sep	623.7±80.4
Sep+GLY	658.5±36.6
Sep-TEMSPU	494.4±39.3
Sep-TEMSPU+GLY	1514.0±88.8
Sep-ClPTES	753.2±66.3
Sep-ClPTES+GLY	740.7±68.3

IC50 (concentration inhibiting 50 % of growth) after exposure in the XTT assay for 24 h. GM07492A cells, normal human lung fibroblasts.

As reported before, the adsorption capacity of functionalized solids was even lower than that of raw sepiolite, and also lower than for other adsorbents reported in the literature (Table 4). However, it is important to underline that the desorption studies show that the selected alkoxides promote the adsorbent-adsorbate interaction and decrease the mobility of the adsorbed contaminants. The stability of the bonds formed with modified sepiolites prevented the removal of contaminant from solids. This could be very interesting in real applications, considering not only the amount adsorbed but also the interaction existing between the specific groups, electrostatic in case of chloropryl group and via hydrogen bond for propylurea.

3.4. Toxicity tests

In a study conducted with organically modified montmorillonite, Sharma et al. [70] pointed out that it is crucial to consider the toxicity of these materials due to the increasing use of clays and organic clays for industrial applications. The cell viability results for GLY, Sep, Sep+GLY, Sep-TEMSPU, Sep-ClPTES, Sep-TEMSPU+GLY and Sep-ClPTES+GLY were used to calculate IC_{50} and are summarized in Table 6. Statistical results for cell viability along the increase in concentration indicated that all samples showed significant differences from the negative control. For GLY and Sep samples, these differences started at concentrations of 2500 and 312.5 μg/mL ($P<0.05$), with IC_{50} of 2262 and 623.7 μg/mL, respectively. Sep-TEMSPU, Sep-ClPTES, Sep-ClPTES+GLY and Sep+GLY concentrations of 625 μg/mL or greater were significantly cytotoxic with $P < 0.05$, with values for IC_{50} of 494.4, 753.2, 740.7, and 658.5 μg/mL, respectively. Sep-TEMSPU+GLY was cytotoxic from 1250 μg/mL ($P<0.05$) and had significantly different IC_{50} (1514 μg/mL) as compared to GLY, pure Sep, Sep+GLY and Sep-TEMSPU. Pure GLY had a high IC_{50} value. As the toxicity test was performed *in vitro*, the molecule did not decompose into its metabolites as in the presence of living organisms. These metabolites, especially aminomethylphosphonic acid (AMPA), are more toxic than the active ingredient and can be found as residues in crop and food products such as fish, as reported by Vera-Candioti et al. [71], who evaluated genotoxicity and cytotoxicity to fish exposed to GLY, and by Guilherme et al. [72], who analyzed the genotoxic effects of the Roundup® trademark on European eel.

The measured IC_{50} for GLY found in this work was 2262 μg/mL. The other samples, pure Sep, Sep + GLY, Sep-ClPTES and Sep-TEMSPU had similar IC_{50} values, ca. 500–700 μg/mL (see Table 6). In general, functionalization did not alter significantly the Sep toxicity. Sep presented toxicity *in vitro*, probably because due to its nanostructure it penetrated the cells and caused their rupture [73]. Sep-TEMSPU behaved differently after adsorption of GLY: Sep-TEMSPU was less toxic, indicating that the adsorption product was less harmful to the environment. The cytotoxicity observed for sample Sep-TEMSPSU + Gly was intermediate between those for sepiolite or Sep + GLY and glyphosate. However, no toxicity difference was observed for Sep-ClPTES after GLY adsorption.

The data obtained showed the low cytotoxicity of glyphosate when bonded to functionalized sepiolite. According to the literature, although some studies have shown a low toxicity of pure glyphosate [74,75], other studies relate the commercial formulations of glyphosate to adverse effects on non-target or collateral organisms. Therefore, it has also been purposed that the toxicity observed in commercial formulations may be related to the presence of surfactants.

4. Conclusions

Sepiolite was successfully functionalized with (3-chloropropyl)triethoxysilane (ClPTES) or 3-[tri(ethoxy/methoxy)silyl] propylurea (TEMSPU) alkoxides. The obtained solids, Sep-ClPTES and Sep- TMSPU, efficiently adsorbed glyphosate (the amount adsorbed decreasing in the order Sep > Sep-ClPTES > Sep-TMSPU) and caffeine (Sep > Sep-TMSPU). Adsorption results evidenced that functional groups blocked the active sites of the adsorbents and suggested that glyphosate and caffeine adsorbed within the zeolitic channels and on the surface of the clay minerals. The differences between chloropropyl and urea groups suggested a steric hindrance promoted by the grafting of the silanes on the surface of the sepiolite fibers. The desorption experiments proved an effective interaction *via* hydrogen bonds between caffeine and glyphosate with urea groups from grafted alkoxide; the adsorbates showed a higher stability on the grafted solids, the effective interactions could lead to lower mobility of the contaminants in the solids. Citotoxicity results evidenced that glyphosate adsorbed on functionalized sepiolite derivatives showed low toxicity.

Declaration of Competing Interest

None.

Acknowledgments

The authors thank a Cooperation Grant jointly financed by Universidad de Salamanca (Spain) and FAPESP (Brazil), reference 2016/50322-2. The Spanish group acknowledges the support from MINECO and ERDF (MAT2016-78863-C2-R), and AG also thanks Santander Bank for funding via the Research Intensification Program. Thanks are given to Dr. Ricardo Furtado for support in biological assays. Brazilian group acknowledges the support from research funding agencies Fundação de Amparo à Pesquisa do Estado de São Paulo, FAPESP (2013/19523-3, 2018/26569-3 and 2017/15482-1), and Coordenação de Aperfeiçoamento de Pessoal de Nível Superior (CAPES-PRINT747059P) and Conselho Nacional de Desenvolvimento Científico e Tecnológico, CNPq (311767/2015-0 and 303135/2018-2). The equipment of Brazilian group has been financed by FAPESP (1998/11022-3, 2005/00720-7, 2011/03335-8, 2012/11673-3 and 2016/01501-1).

Supplementary materials

Supplementary material associated with this article can be found, in the online version, at doi:10.1016/j.apsadv.2020.100025.

References

[1] H. Ali, E. Khan, Environmental chemistry in the twenty-first century, Environ. Chem. Lett. 15 (2017) 329–346, doi:10.1007/s10311-016-0601-3.
[2] B. Fernández-Reyes, K. Ortiz-Martínez, J.A. Lasalde-Ramírez, A.J. Hernández-Maldonado, Engineered adsorbents for the removal of contaminants of emerging concern from water, Chapter 1, in: A.J. Hernández-Maldonado, L. Blaney (Eds.), Contaminants of Emerging Concern in Water and Wastewater, Butterworth-Heinemann, 2020, doi:10.1016/B978-0-12-813561-7.00001-8.
[3] T. Rasheed, M. Bilal, F. Nabeel, M. Adeel, H.M.N. Iqbal, Environmentally-related contaminants of high concern: potential sources and analytical modalities for detection, quantification, and treatment, Environ. Int. 122 (2019) 52–66, doi:10.1016/j.envint.2018.11.038.

[4] D.D. Snow, D.A. Cassada, Larsen M.L., N.A. Mware, X. Li, M. D'Alessio, Y. Zhang, J.B. Sallach, Detection, occurrence and fate of emerging contaminants in agricultural environments, Water Environ. Res. 89 (2017) 897–920, doi:10.2175/106143017X15023776270160.

[5] J. Xu, S. Smith, G. Smith, W. Wang, Y. Li, Glyphosate contamination in grains and foods: an overview, Food Control 106 (2019) 106710, doi:10.1016/j.foodcont.2019.106710.

[6] M.T. Rose, T.R. Cavagnaro, C.A. Scanlan, T.J. Rose, T. Vancov, S. Kimber, I.R. Kennedy, R.S. Kookana, L.V. Zwieten, Impact of herbicides on soil biology and function, in: D.L. Sparks (Ed.), Advances in Agronomy, 136, Elsevier, 2016, pp. 133–220.

[7] L.P. Agostini, R.S. Dettogni, R.S. Reis, E. Stur, E.V.W. dos Santos, D.P. Ventorim, F.M. Garcia, R.C. Cardoso, J.B. Graceli, I.D. Louro, Effects of glyphosate exposure on human health: Insights from epidemiological and in vitro studies, Sci. Total Environ. 705 (2020) 135808, doi:10.1016/j.scitotenv.2019.135808.

[8] L. Pollegioni, E. Schonbrunn, D. Siehl, Molecular basis of glyphosate resistance-different approaches through protein engineering, FEBS J. 278 (2011) 2753–2766, doi:10.1111/j.1742-4658.2011.08214.x.

[9] M. Sun, H. Li, D.P. Jaisi, Degradation of glyphosate and bioavailability of phosphorus derived from glyphosate in a soil-water system, Water Res. 163 (2019) 114840, doi:10.1016/j.watres.2019.07.007.

[10] O. Borggaard, A.L. Gimsing, Fate of glyphosate in soil and the possibility of leaching to ground and surface waters: a review, Pest Manag. Sci. 64 (2008) 441–456, doi:10.1002/ps.1512.

[11] M.J. Shipitalo, L.B. Owens, Comparative losses of glyphosate and selected residual herbicides in surface runoff from conservation-tilled watersheds planted with corn or soybean, J. Environ. Qual. 40 (2011) 1281–1289, doi:10.2134/jeq2010.0454.

[12] J.P. Giesy, S. Dobson, K.R. Solomon, Ecotoxicological risk assessment for roundup® herbicide, in: G.W. Ware (Ed.), Reviews of Environmental Contamination and Toxicology, 167, Springer, 2000, doi:10.1007/978-1-4612-1156-3_2.

[13] J. Sanchís, L. Kantiani, M. Llorca, F. Rubio, A. Ginebreda, J. Fraile, T. Garrido, M. Farré, Determination of glyphosate in groundwater samples using an ultrasensitive immunoassay and confirmation by on-line solid-phase extraction followed by liquid chromatography coupled to tandem mass spectrometry, Anal. Bioanal. Chem. 402 (2012) 2335–2345, doi:10.1007/s00216-011-5541-y.

[14] World Health Organization, Glyphosate. International Programme on Chemical Safety. Environmental Health Criteria, 159 (1994).

[15] S. Qiu, H. Fu, R. Zhou, Z. Yang, G. Bai, B. Shi, Toxic effects of glyphosate on intestinal morphology, antioxidant capacity and barrier function in weaned piglets, Ecotox. Environ. Saf. 187 (2020) 109846, doi:10.1016/j.ecoenv.2019.109846.

[16] J. Zhao, S. Pacenka, J. Wu, B.K. Richards, T. Steenhuis, K. Simpson, A.G. Hay, Detection of glyphosate residues in companion animal feeds, Environ. Pollut. 243 (2018) 1113–1118, doi:10.1016/j.envpol.2018.08.100.

[17] R.R.N. Marques, M.J. Sampaio, P.M. Carrapiço, C.G. Silva, S. Morales-Torres, G. Dražić, J.L. Faria, A.M.T. Silva, Photocatalytic degradation of caffeine: developing solutions for emerging pollutants, Catal. Today 209 (2013) 108–115, doi:10.1016/j.cattod.2012.10.008.

[18] L. Marçal, E.H. de Faria, E.J. Nassar, R. Trujillano, N. Martín, M.A. Vicente, V. Rives, A. Gil, S.A. Korili, K.J. Ciuffi, Organically modified saponites: SAXS study of swelling and application in caffeine removal, ACS Appl. Mater. Interfaces 7 (2015) 10853–10862, doi:10.1021/acsami.5b01894.

[19] S. Li, B. He, J. Wang, J. Liu, X. Hu, Risks of caffeine residues in the environment: necessity for a targeted ecopharmacovigilance program, Chemosphere 243 (2020) 125343, doi:10.1016/j.chemosphere.2019.125343.

[20] M. Bandookwala, A.K. Sahu, D. Thakkar, M. Sharma, A. Khairnar, P. Sengupta, Edaravone-caffeine combination for the effective management of rotenone induced Parkinson's disease in rats: an evidence based affirmative from a comparative analysis of behavior and biomarker expression, Neurosci. Lett. 711 (2019) 134438, doi:10.1016/j.neulet.2019.134438.

[21] J. Watson, Caffeine, in: B. Caballero (Ed.), Encyclopedia of Food Sciences and Nutrition, Second ed., Elsevier, 2003, pp. 745–750.

[22] G. Zhuang, J. Gao, H. Chen, Z. Zhang, A new one-step method for physical purification and organic modification of sepiolite, Appl. Clay Sci. 153 (2018) 1–8, doi:10.1016/j.clay.2017.11.045.

[23] M.S. del Río, E. García-Romero, M. Suárez, I. da Silva, L. Fuentes-Montero, G. Martínez-Criado, Variability in sepiolite: diffraction studies, Am. Miner. 96 (2011) 1443–1454, doi:10.2138/am.2011.3761.

[24] Z. Li, A. Gómez-Avilés, L. Sellaoui, J. Bedia, A. Bonilla-Petriciolet, C. Belver, Adsorption of ibuprofen on organo-sepiolite and on zeolite/sepiolite heterostructure: synthesis, characterization and statistical physics modeling, Chem. Eng. J. 371 (2019) 868–875, doi:10.1016/j.cej.2019.04.138.

[25] G. Lagaly, M. Ogawa, I. Dékány, Clay mineral–organic interactions, chapter 10.3, in: F. Bergaya, G. Lagaly (Eds.), Handbook of clay science, 5, Elsevier, 2013, pp. 435–505. Developments in Clay Science, doi:10.1016/B978-0-08-098258-8.00015-8.

[26] M.A. Moreira, K.J. Ciuffi, V. Rives, M.A. Vicente, R. Trujillano, A. Gil, S. Korili, E.H. de Faria, Effect of chemical modification of palygorskite and sepiolite by 3-aminopropyltriethoxisilane on adsorption of cationic and anionic dyes, Appl. Clay Sci. 135 (2017) 394–404, doi:10.1016/j.clay.2016.10.022.

[27] M. Doğan, Y. Turhan, M. Alkan, H. Namli, P. Turan, Ö. Demirbaş, Functionalized sepiolite for heavy metal ions adsorption, Desalination 230 (2008) 248–268, doi:10.1016/j.desal.2007.11.029.

[28] A.J. Aznar, J. Sanz, E. Ruiz-Hiztky, Mechanism of the grafting of organosilanes on mineral surfaces. IV. Phenylderivatives of sepiolite and poly (organosiloxanes), Colloid Polym. Sci. 270 (1992) 165–176, doi:10.1007/BF00652183.

[29] K.A. Carrado, L. Xu, R. Csencsits, J.V. Muntean, Use of organo- and alkoxysilanes in the synthesis of grafted and pristine clays, Chem. Mater. 13 (2001) 3767–3773, doi:10.1021/cm010104o.

[30] E. Bilotti, R. Zhang, H. Deng, F. Quero, H.R. Fischer, T. Peijs, Sepiolite needle-like clay for PA6 nanocomposites: An alternative to layered silicates? Compos. Sci. Technol. 69 (2009) 2587–2595, doi:10.1016/j.compscitech.2009.07.016.

[31] N. García, J. Guzman, J. Benito, A. Esteban-Cubillo, E. Aguilar, J. Santander, P. Tiemblo, Surface modification of sepiolite in aqueous gels by using methoxysilanes and its impact on the nanofiber dispersion ability, Langmuir 27 (2011) 3952–3959, doi:10.1021/la104410r.

[32] K.O. Moura, H. Pastore, Physico-chemical of organo-functionalized magnesium phyllosilicate prepared by microwave heating, Micropor. Mesopor. Mater. 190 (2014) 292–300, doi:10.1016/j.micromeso.2014.02.027.

[33] F. Rouquerol, J. Rouquerol, K. Sing, Adsorption by powders and porous solids, Principles, Methodology and Applications, Academic Press, 1999.

[34] M. Alkan, S. Çerlikçapa, Ö. Demirbas, M. Dogan, Removal of reactive blue 221 and acid blue 62 anionic dyes from aqueous solutions by sepiolite, Dyes Pigments 6 (2005) 251–259, doi:10.1016/j.dyepig.2004.07.018.

[35] T. Brody, Drug-drug interaction: part one (Small molecule drugs), Chapter 7 in FDA's Drug Review Process and the Package Label: Strategies for Writing Successful FDA Submissions, 1st ed., Academic Press, 2017.

[36] P.K. Gupta, Illustrated Toxicology: With Study Questions (Chapter 1), 1st ed., Elsevier, 2018.

[37] E. Ymele, Z.L.S. Jiokeng, T.M.M. Francis, I.K. Tonle, Nanohybrid materials from amine functionalization of sepiolite: preparation, characterization and application as electrode modifiers for the electroanalytical detection of heavy metal ions, Adv. Mater. Sci. 2 (2017) 1–8, doi:10.15761/AMS.1000133.

[38] M. Thommes, K. Kaneko, A.V. Neimark, J.P. Olivier, F. Rodríguez-Reinoso, J. Rouquerol, K.S.W. Sing, Physisorption of gases, with special reference to the evaluation of surface area and pore size distribution (IUPAC Technical Report), Pure Appl. Chem. 87 (2015) 1051–1069, doi:10.1515/pac-2014-1117.

[39] E. Eren, O. Cubuk, H. Ciftci, B. Eren, B. Caglar, Adsorption of basic dye from aqueous solutions by modified sepiolite: Equilibrium, kinetics and thermodynamics study, Desalination 252 (2010) 88–96, doi:10.1016/j.desal.2009.10.020.

[40] M. Akkari, P. Aranda, A. Mayoral, M. García-Hernández, A. Ben Haj Amara, E. Ruiz-Hitzky, Sepiolite nanoplatform for the simultaneous assembly of magnetite and zinc oxide nanoparticles as photocatalyst for improving removal of organic pollutants, J. Hazard Mater. 340 (2017) 281–290, doi:10.1016/j.jhazmat.2017.06.067.

[41] M. Alkan, G. Tekin, H. Namli, FTIR and zeta potential measurements of sepiolite treated with some organosilanes, Micropor. Mesopor. Mater. 84 (2005) 75–83, doi:10.1016/j.micromeso.2005.05.016.

[42] R.L. Frost, E. Mendelovici, Modification of fibrous silicates surfaces with organic derivatives: an infrared spectroscopic study, J. Colloid Interface Sci. 294 (2006) 47–52, doi:10.1016/j.jcis.2005.07.014.

[43] F. Adam, H. Osman, K.M. Hello, The immobilization of 3-(chloropropyl)triethoxysilane onto silica by a simple one-pot synthesis, J. Coll. Interface Sci. 331 (2009) 143–147, doi:10.1016/j.jcis.2008.11.048.

[44] J. Madejová, W.P. Gates, S. Petit, IR spectra of clay minerals. Infrared and Raman spectroscopies of clay mineral, Dev. Clay Sci. 8 (2017) 107–149.

[45] R.C. MacKenzie, Differential thermal analysis, Fundamental Aspects, 1, Academic Press, 1970.

[46] R.L. Frost, J. Kristóf, E. Horváth, Controlled rate thermal analysis of sepiolite, J. Therm. Anal. 98 (2009) 749–755, doi:10.1007/s10973-009-0321-z.

[47] H. Chen, D. Zeng, X. Xiao, M. Zheng, C. Ke, Y. Li, Influence of organic modification on the structure and properties of polyurethane/sepiolite nanocomposites, Mater. Sci. Eng. A – Struct. 528 (2011) 1656–1661, doi:10.1016/j.msea.2010.10.087.

[48] M. Suárez, E. García-Romero, Variability of the surface properties of sepiolite, Appl. Clay Sci. 67–68 (2012) 72–82, doi:10.1016/j.clay.2012.06.003.

[49] S. Lazarević, I. Janković-Častvan, D. Jovanović, S. Milonjić, D. Janaćković, R. Petrović, Adsorption of Pb^{2+}, Cd^{2+} and Sr^{2+} ions onto natural and acid-activated sepiolites, Appl. Clay Sci. 37 (2007) 47–57, doi:10.1016/j.clay.2006.11.008.

[50] M. Kragović, M. Stojmenović, J. Petrović, J. Loredo, S. Pašalić, A. Nedeljković, I. Ristović, Influence of alginate encapsulation on point of zero charge (pHpzc) and thermodynamic properties of the natural and Fe(III) – modified zeolite, Procedia Manuf. 32 (2019) 286–293, doi:10.1016/j.promfg.2019.02.216.

[51] J.-B. Le, J. Cheng, Modeling electrochemical interfaces from ab initio molecular dynamics: water adsorption on metal surfaces at potential of zero charge, Curr. Opin. Electrochem. 19 (2020) 129–136, doi:10.1016/j.coelec.2019.11.008.

[52] C.F.B. Coutinho, L.H. Mazo, Complexos metálicos com o herbicida glifosato: revisão, Quím. Nova 28 (2005) 1038–1045, doi:10.1590/S0100-40422005000600019.

[53] L. Marçal, E.H. de Faria, M. Saltarelli, P.S. Calefi, E.J. Nassar, K.J. Ciuffi, R. Trujillano, M.A. Vicente, S.A. Korili, A. Gil, Amine-functionalized titanosilicates prepared by the sol–gel process as adsorbents of the azo-dye orange II, Ind. Eng. Chem. Res. 50 (2011) 239–246, doi:10.1021/ie101650h.

[54] A.M. Awad, S.M.R. Shaikh, R. Jalab, M.H. Gulied, M.S. Nasser, A. Benamor, S. Adham, Adsorption of organic pollutants by natural and modified clays: a comprehensive review, Sep. Purif. Technol. 228 (2019) 115719, doi:10.1016/j.seppur.2019.115719.

[55] L. Santamaría, M. López-Aizpún, M. García-Padial, M.A. Vicente, S.A. Korili, A. Gil, Zn-Ti-Al layered double hydroxides synthesized from aluminum saline slag wastes as efficient drug adsorbents, Appl. Clay Sci. 187 (2020) 105486, doi:10.1016/j.clay.2020.105486.

[56] A. Gil, L. Santamaría, S.A. Korili, Removal of caffeine and diclofenac from aqueous solution by adsorption on multiwalled carbon nanotubes, Colloid Interface Sci. Commun. 22 (2018) 25–28, doi:10.1016/j.colcom.2017.11.007.

[57] A. Khenifi, Z. Derriche, C. Mousty, V. Prévot, C. Forano, Adsorption of Glyphosate and Glufosinate by Ni_2AlNO_3 layered double hydroxide, Appl. Clay Sci. 47 (2010) 362–371, doi:10.1016/j.clay.2009.11.055.
[58] F. Li, Y. Wang, Q. Yang, D.G. Evans, C. Forano, X. Duan, Study on adsorption of glyphosate (N-phosphonomethyl glycine) pesticide on MgAl-layered double hydroxides in aqueous solution, J. Hazard. Mater. 125 (2005) 89–95, doi:10.1016/j.jhazmat.2005.04.037.
[59] C.H. Giles, D. Smith, A. Huitson, A general treatment and classification of the solute adsorption isotherm. I. Theoretical, J. Colloid Interface Sci. 47 (1974) 755–765, doi:10.1016/0021-9797(74)90252-5.
[60] D.D. Do, Adsorption Analysis: Equilibria and Kinetics, Imperial College Press, 1998.
[61] E. Morillo, T. Undabeytia, C. Maqueda, A. Ramos, Glyphosate adsorption on soils of different characteristics: Influence of copper addition, Chemosphere 40 (2000) 103–107, doi:10.1016/S0045-6535(99)00255-6.
[62] N. Ayawei, A.N. Ebelegi, D. Wankasi, Modelling and interpretation of adsorption isotherms, J. Chem. (2017) (2017) 3039817, doi:10.1155/2017/3039817.
[63] R.T.A. Carneiro, T.B. Taketa, R.J. Gomes Neto, J.L. Oliveira, E.V.R. Campos, M.A. de Moraes, C.M.G. da Silva, M.M. Beppu, L.F. Fraceto, Removal of glyphosate herbicide from water using biopolymer membranes, J. Environ. Manag. 151 (2015) 353–360, doi:10.1016/j.jenvman.2015.01.005.
[64] Y.S. Hu, Y.Q. Zhao, B. Sorohan, Removal of glyphosate from aqueous environment by adsorption using water industrial residual, Desalination 271 (2011) 150–156, doi:10.1016/j.desal.2010.12.014.
[65] S.S. Mayakaduwa, P. Kumarathilaka, I. Herath, M. Ahmad, Al-Wabel M., Y.S. Ok, A. Usman, A. Abduljabbar, M. Vithanage, Equilibrium and kinetic mechanisms of woody biochar on aqueous glyphosate removal, Chemosphere 144 (2016) 2516–2521, doi:10.1016/j.chemosphere.2015.07.080.
[66] M. Milojević-Rakić, A. Janošević, J. Krstić, B. Nedić Vasiljević, V. Dondur, G. Ćirić-Marjanović, Polyaniline and its composites with zeolite ZSM-5 for efficient removal of glyphosate from aqueous solution, Micropor. Mesopor. Mater. 180 (2013) 141–155, doi:10.1016/j.micromeso.2013.06.025.
[67] E. Morillo, T. Undabeytia, C. Maqueda, Adsorption of glyphosate on the clay mineral montmorillonite: effect of Cu(II) in solution and adsorbed on the mineral, Environ. Sci. Technol. 31 (1997) 3588–3592, doi:10.1021/es970341l.
[68] Y.S. Hu, Y.Q. Zhao, B. Sorohan, Removal of glyphosate from aqueous environment by adsorption using water industrial residual, Desalination 271 (2011) 150–156, doi:10.1016/j.desal.2010.12.014.
[69] A. Piccolo, G. Celano, M. Arienzo, A. Mirabella, Adsorption and desorption of glyphosate in some European soils, J. Environ. Sci. Heal. B 29 (1994) 1105–1115, doi:10.1080/03601239409372918.
[70] A.K. Sharma, A. Mortensen, B. Schmidt, H. Frandsen, N. Hadrup, E.H. Larsen, M.-L. Binderup, In-vivo study of genotoxic and inflammatory effects of the organo-modified montmorillonite Cloisite® 30B, Mutat. Res. Genet. Toxicol. Environ. Mutagen. 770 (2014) 66–71, doi:10.1016/j.mrgentox.2014.04.023.
[71] J. Vera-Candioti, S. Soloneski, M.L. Larramendy, Evaluation of the genotoxic and cytotoxic effects of glyphosate-based herbicides in the ten spotted live-bearer fish *Cnesterodon decemmaculatus* (Jenyns, 1842), Ecotox. Environ. Saf. 89 (2013) 166–173, doi:10.1016/j.ecoenv.2012.11.028.
[72] S. Guilherme, M.A. Santos, I. Gaivão, M. Pacheco, Are DNA-damaging effects induced by herbicide formulations (Roundup® and Garlon®) in fish transient and reversible upon cessation of exposure? Aquat. Toxicol. 155 (2014) 213–221, doi:10.1016/j.aquatox.2014.06.007.
[73] S. Maisanaba, S. Pichardo, M. Puerto, D. Gutiérrez-Praena, A.M. Cameán, A. Jos, Toxicological evaluation of clay minerals and derived nanocomposites: a review, Environ. Res. 138 (2015) 233–254, doi:10.1016/j.envres.2014.12.024.
[74] C.M. Howe, M. Berrill, B.D. Pauli, C.C. Helbing, K. Werry, N. Veldhoen, Toxicity of glyphosate-based pesticides to four North American frog species, Environ. Toxicol. Chem. 23 (2004) 1928–1938, doi:10.1897/03-71.
[75] F. Peixoto, Comparative effects of the roundup and glyphosate on mitochondrial oxidative phosphorylation, Chemosphere 61 (2005) 1115–1122, doi:10.1016/j.chemosphere.2005.03.044.